Naproxen sodium salt photochemistry in aqueous sodium dodecyl sulfate (SDS) ellipsoidal micelles

M.Valero*[a], Natalya. B. Sultimova[b], Judith E. Houston[c,d] , Peter P. Levin[b,e]

[a] Dpto. Química Física, Facultad de Farmacia, Universidad de Salamanca, Campus Miguel de Unamuno, s/n, 37007 Salamanca, Spain

[b] Emanuel Institute of Biochemical Physics, Russian Academy of Sciences, Moscow, Russia, 119334.

[c] Jülich Centre for Neutron Science (JCNS) at Heinz Maier-Leibnitz Zentrum (MLZ) Forschungszentrum Jülich GmbH, Lichtenbergstraße 1, 85747 Garching, Germany.

[d] European Spallation Source (ESS), Odarslövsvägen 113, 225 92 Lund, Sweden.

[e] Semenov Institute of Chemical Physics, Russian Academy of Sciences, Moscow, Russia, 119334.

Abstract

The photochemistry and other properties of the anti-inflammatory drug (NSAID) naproxen (NP) in sodium dodecyl sulfate, SDS, micellar aqueous solutions at pH = 7 (NP is in anionic form) were studied. The large value of the partition coefficient (P) was obtained, logP = 2.7, showing that the most part of NP is localized in the micellar phase. The solubilization in SDS micelles results in NP fluorescence and photodegradation quantum yields decrease. The photoproducts 6-methoxy-2-(1-hydroxyethyl)-naphthalene and 6-methoxy-2-acetyl-naphthalene were found by gas chromatography/mass spectrometry (GC/MS). Both photoproducts were formed in SDS solution in significantly smaller amounts than in water. Small angle neutron scattering (SANS) showed that the presence of NP has small effect on the micellar structure. Only a slight decrease of the ionization degree of the micelle was observed by SANS, suggesting that NP was localized in the vicinity of micellar surface. The NP triplet excited state, hydrated electron, NP radical cation and some other relatively long lived intermediate were observed by laser flash photolysis of NP in micellar solution. The decay kinetics of these intermediates was different with respect to that in the homogeneous media.

ABBREVIATIONS
NP: Naproxen
NB: Nabumetone
NSAID: non-steroidal anti-inflammatory drug
SDS: sodium dodecylsulfate
SANS: small angle neutron scattering
GC/MS: gas chromatography/mass spectrometry
LFP: laser flash photolysis

The reactivity of NP in SDS micellar environment was compared to that in the homogeneous media and the probable nature of the intermediate precursors of the final photoproducts are under the discussion.

Key words

Naproxen sodium salt, sodium dodecyl sulfate (SDS), micelles, small angle neutron scattering (SANS), photochemistry, fluorescence, laser flash photolysis.

1. Introduction

Naproxen (NP) (**(1)** in Scheme 1) is a nonsteroidal anti-inflammatory drug (NSAID) available over the counter used to alleviate moderate pain, fever and inflammatory diseases. It was one of the most commonly prescribed medication in the United States, with more than eleven million prescriptions [1,2]. NP, as many other drugs of high consume by humans, has been detected in aqueous reservoirs [3] and, despite it is often below the limit of quantification, in living beings [4].

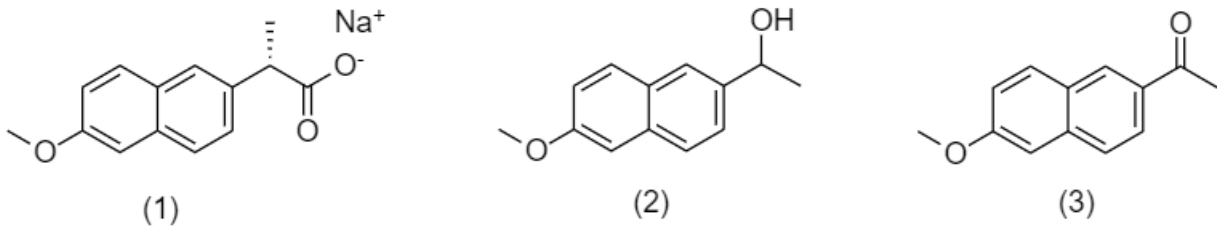

Scheme 1: Chemical structure of: **(1)** anionic form of naproxen (**NP**) (sodium -2-(6-methoxynaphthalen-2-yl) propanoate and the photoproducts: **(2)** (6-methoxy-2-(1-hydroxyethyl) naphthalene, and **(3)** 6-methoxy-2-acetyl-naphthalene.

As other members of the family, NP is a well-known photosensitizing agent. Its photophysical and photochemical behavior has been studied in homogeneous media of different polarity [5–10]. Some scare data are available also for heterogeneous media, such as cyclodextrins (CDs), [11–13] and micellar aggregates, namely anionic sodium dodecyl sulfate (SDS) [7,11] and cationic cetyl trimethyl ammonium bromide (CTAB) [7].

The ionized form of NP (compound (1) in Scheme 1) has been studied in aqueous media [7,8,14] and other homogeneous media like ethanol [8] or acetonitrile [9]. These studies describe the intermediates involved in the photodegradation process as well as the final photoproducts. Whereas, in the heterogeneous hydrophobic environments the only aspects studied are the photomixture composition [11–13] or the singlet oxygen formation [7] after light irradiation of the drug. However, the ionized NP form can be accumulated in membranes [15], where photosensitizing effects produced by the drug are expected. Therefore, the investigation of NP photochemical behavior in restricted biological media would afford useful information about its bioaccumulation and phototoxicological effects in the patients treated,

and also in living organisms, plants or animals, that can get in contact with them in the water reservoirs or by means of these aquatic species through the trophic chain.

SDS micelles have been demonstrated to be an appropriate biomimetic model [16,17]. It is well known that micelles and other restricted environments can act as supercages where the reactivity of the chemicals is changed in a specific way. The micellar aggregates either prevent the photodegradation of pharmaceuticals and natural compounds [18–20] or can promote the photodegradation of chemical contaminants presented in the water pools [18,20,21]. Interestingly, recent works showed that SDS aggregates protect the NSAID nabumetone (NB) against the photodegradation [17]. Therefore, we are curious about whether the SDS protection activity works with NSAIDs of different structure.

For all these reasons, the aim of the present work was to study the photophysical and photochemical behavior of the ionized NP in aqueous SDS micellar solutions. We have used uv-vis absorption and fluorescence techniques to determine the drug distribution in the micelle/water system and photodegradation kinetics. Small angle neutron scattering (SANS) was used to examine the effect of drug presence on the micellar structure. Gas Chromatography/Mass Spectrometry (GC/MS) and laser flash photolysis (LFP) gave the information about final and intermediate photoproducts.

The results obtained show that despite the negative charge of the aggregate surface, the most part of ionized NP is accumulated in the micellar phase. So the SDS micelle allows the study of the photochemical behavior of the ionized NP in a restricted hydrophobic medium, carried out for the first time.

Anionic NP photoirradiation in aqueous SDS micellar solution gives rise to the same photoproducts as were detected previously in the most of the homogeneous media but in lower amount. The protection afforded by SDS micelle to NP from the light is due to the micellar stabilization of the radicals involved in the NP photoproducts formation. If to compare the photochemical behavior of NP with that of the structural related NSAID NB [17], it is possible to speculate that in both cases SDS is acting as the source of the hydrogen atoms needed to initially form reduced photoproducts. Nonetheless, the oxidation rate of the alcoholic photoproduct (2) of NP to form the photoproduct (3) was found to increase in SDS.

By contrast to the previous studies, the photodegradation of the ionic NP is suggested to be from the ^{3}NP and not from the ^{1}NP, as most commonly invoked [5]. Fundamental insights into the probable mechanisms of the photoproducts formation are also obtained.

From a practical point of view, the outcomes suggest the possibility of bioaccumulation of the drug in hydrophobic domains of aquatic organisms by topical contact. The lower photoreactivity in the micelles than in water is a hopeful result from toxicological point of view, but it alerts about the undesirable increase of the persistence of pharmaceuticals in aqueous pools due to the presence of surfactants, which are also frequent contaminants of the aqueous media, coming from the health care products [22].

2. Experimental section

2.1. Materials

Naproxen sodium salt, (NP, M1275), was obtained from Sigma. Naproxen in molecular form (NP, C15483500), 99.6% of purity, was purchased from Dr Ehrenstorfer, GmbH. Sodium dodecyl sulfate, (SDS, 230425000) for biochemistry, 99% purity, was purchased from Agros Organic. HCl was from Sigma. The chemicals were used as received.

For the preparation of the samples for SANS measurements, D_2O (Sigma-Aldrich, 99.8% purity) was used instead of water. For all other experiments, samples were prepared with ultrapure water (18.2 MΩ·cm, Millipore-filtered).

2.2. Solutions

Aqueous stock solutions of (1) SDS 0.2 M, (2) NP, 1mM and (3) NP 1 mM and SDS 0.2M, were initially prepared under mechanical stirring. The solutions with different concentrations of NP and SDS were obtained by mixing appropriate amounts of the stock solutions.

For NP solubility determination, fixed volume of the aqueous solutions with different SDS concentration, in the range of 0-0.2 M, prepared by diluting solution (1) was added to an excess of molecular NP weighted in a topaz vial. The pH was modified by adding the appropriate amount of HCl concentrated solution.

For SANS, a stock solution of SDS 0.2M in D_2O was prepared. 1 mM NP in D_2O or in 0.2 M SDS solutions in D_2O were prepared by sodium salt of the drug weighing and solubilizing.

Irradiated solutions of 1 mM NP in water and in 0.2 M SDS aqueous solutions were analyzed by GC/MS.

Except for solubility measurements, sodium salt of naproxen was used, then the samples have pH=7.

2.3. Methods

2.3.1. Uv-Vis Absorption and Emission Spectroscopies

In the solubility determination, solutions were subjected to a 72h of mechanical stirring in a dark room at 20ºC. Saturated solutions were centrifuged in a Centrolit P-Selecta, with a max 12000 rpm, during 10 min. The supernatant was then diluted with water or SDS solution of the appropriate concentration, then NP concentration was determined by uv-vis absorption spectroscopy.

Measurements were performed on UV-Vis Hitachi, model 150-20, spectrophotometer. Absorption spectrum was obtained in the range λ = 250-450 nm, in a quartz cuvette with 1cm pathlength, using Milli Q water as a reference. NP absorption spectrum shows characteristics bands systems centered at 317, 330 nm [23–25]. The SDS addition does not produce any

spectral shift but does some variation of the NP absorbance (S1). NP concentration was determined from the value of A_{330}.

The extinction coefficient of the samples, at each pH in H_2O and SDS, was experimentally determined using Eq.1.

$$\varepsilon_{p^H}^{medium} = \alpha * \varepsilon_{NP^-}^{medium} + (1-\alpha) * \varepsilon_{NPH}^{medium} \quad \text{Eq. (1)}$$

Where α is the ionization degree of the drug at each pH, determined considering the aqueous pKa= 4.15 [26]; and ε is the corresponding molar absorptivity of each species, NP^- and NPH, in H_2O or aqueous SDS, experimentally determined (S2).

SDS volume fraction (ϕ_{SDS}) was calculated using SDS molar volume, $\bar{V}_{SDS}$ =0.288 L/mol [27].

Steady-state fluorescence emission and excitation spectra were recorded with a Perkin Elmer LS 50B spectrofluorimeter with the thermostated sample holder. The spectra were corrected using software provided with the apparatus.

The emission spectra were obtained with excitation wavelength λ_{exc}= 317 nm in emission wavelength range λ_{em}= 325-450 nm.

The fluorescence quantum yields, Φ_f, were measured as described elsewhere [28] using the reference quantum yield (0.543) for quinine sulfate in 0.1N sulfuric acid [29].

2.3.2. Small-Angle Neutron Scattering (SANS)

SANS experiments were carried out on the KWS-2 diffractometer at the Jülich Centre for Neutron Science (JCNS), Münich, Germany [30]. An incident radiation wavelength of 5 Å was used with detector distances of 1.7 and 7.6 m and a collimation length of 8 m, to cover a momentum transfer, q, range from 0.008 to 0.5 $Å^{-1}$. In the standard mode, a wavelength spread $\Delta\lambda/\lambda$= 20% was used. All samples were measured in quartz cells (Hellma) with a path length of 2 mm using D_2O as the solvent. The samples were placed in an aluminum rack where water was recirculated from an external Julabo cryostat, at 25 ºC. This set-up enables a thermal control with up to 0.1 ºC precision. Scattered intensities were corrected for detector pixel efficiency, empty cell scattering and background due to electronic noise. The data were set to absolute scale using Plexiglas as a secondary standard. The obtained macroscopic differential cross-section $d\Sigma/d\Omega$ was further corrected for the contribution from the solvent. The complete data processing was performed with the QtiKWS software provided by JCNS in Garching [30].

Solutions of SDS with two concentrations (0.05 and 0.2 M) without and with 1 mM of NP were studied. All samples were measured in D_2O in order to optimize the contrast and minimize the incoherent background in SANS experiments.

SANS curves were fitted using SAS View 4.2.1. software to an ellipsoid model [31,32] with a Hayter-Penfold MSA interparticle structure factor S(Q) for charged particles. The parameter $sld_{SDS\ micelle}$=0.337 × 10^{-6} Å^{-2}, a dielectric constant of D_2O =77.936 [33] and the scale factor equal to 1, were fixed.

The aggregation number (N_{agg}) was determined as described in [34].

2.3.3. Photodegradation

Heraeus Noblelight photoreactor, with UV immersion lamp TQ 150 (high pressure mercury lamp), with emission maxima at λ = 365 nm and 313 nm (with lower intensity), was used to irradiate the solutions.

The wavelength of the radiation implicated in the most of the phototoxic processes was in the range from 300 to 400 nm [35]. Because of that, the use of a mercury lamp radiating in the absorption region of both the initial NP and the photolysis products seemed to be reasonable.

The incident light intensity (I_0) was detected by a potassium ferrioxilate actinometer solution (0.006 M). The photodegradation quantum yield at the emission wavelengths of the lamp are ϕ_{365} =1.21 and ϕ_{313} =1.24 [36]. Assuming total light absorption by the actinometer [37] and using the method described elsewhere [35]. The total intensity of the irradiating lamp was 4.15 × 10^{-6} Einstein L^{-1} s^{-1}. NP absorption spectra in water and SDS (S1) show that the drug absorbs at λ=313 nm whereas the absorption at 365 nm is negligible. Since the intensity at 365 nm is 1.73 times higher than at 313 nm, as stated by the manufacturer, the estimated light intensity of the lamp at 313 nm was 1.52 × 10^{-6} Einstein L^{-1} s^{-1}.

The phototodegradation quantum yield of NP, ϕ_{PD}, was calculated from the experimental photodegradation rate constant, $k_{PD,}$ as described in [38], using the characteristics of the photoreactor provided by the manufacturer.

2.3.4. Gas Chromatography /Mass Spectrometry (GC/MS)

GC/MS analysis was made with an Agilen 7890A gases chromatograph. Agilent MS220 masses detector was equipped with a VF-5MS column (30 m length x 0.25 mm inner diameter with 0.25 μm stationary phase thickness).

GC temperature was: injector temperature, 270º; interface temperature 290º; furnace temperature was held at 50º for 5 min, to 270ºC at 10ºC/min and held for 5 min. Mass detection realized by monitoring the masses between 50-500 amu.

2.3.5. Flash Photolysis

The absorption spectra and the decay kinetics of intermediates were measured using the nanosecond laser photolysis apparatus with the registration of UV-Vis absorption kinetics at a given wavelength in the range 400 – 800 nm [39,40].

Nitrogen laser (PRA LN 1000, with 1 ns pulse duration and 337 nm radiation wavelength, operating in the 10 Hz frequency mode) was used as an excitation source. Acquisition and averaging of kinetic curves were performed by UF258 transient recorder for PCI bus connected with a personal computer. Each experimental kinetic curve contained 12–14 bits of points with the distance between points being 2–400 ns. Dissolved air oxygen was removed by Ar bubbling during 20 min. All measurements were carried out in a quartz cell with an optical path length of 2 mm at 20 °C.

3. Results and Discussion

3.1. Naproxen in Aqueous SDS Solution.

The aqueous solutions of NP and SDS were characterized by fluorescence and absorption uv-vis spectroscopies, as well as by small angle neutron scattering (SANS). Uv-vis spectroscopies give information about the drug and SANS does it about the aggregate.

3.1.1. Steady-State Fluorescence of NP in Aqueous SDS Solutions

The effect of SDS concentration, varied in a range 0-0.2 M, on NP fluorescence (FL) was studied at two drug concentrations, 0.04 and 1 mM.

NP presents an emission maximum centered at 355 nm in water [28]. At both drug concentrations, SDS addition results in a quenching of fluorescence (Figure 1), showing that NP is passing from the aqueous to the micellar phase in spite of the negative charges of the drug and the micellar surface. The most probable location of the drug in the aggregate is close to the micelle surface, with the aromatic ring in contact to the hydrophobic tails and the carboxylic group nearby the micelle surface.

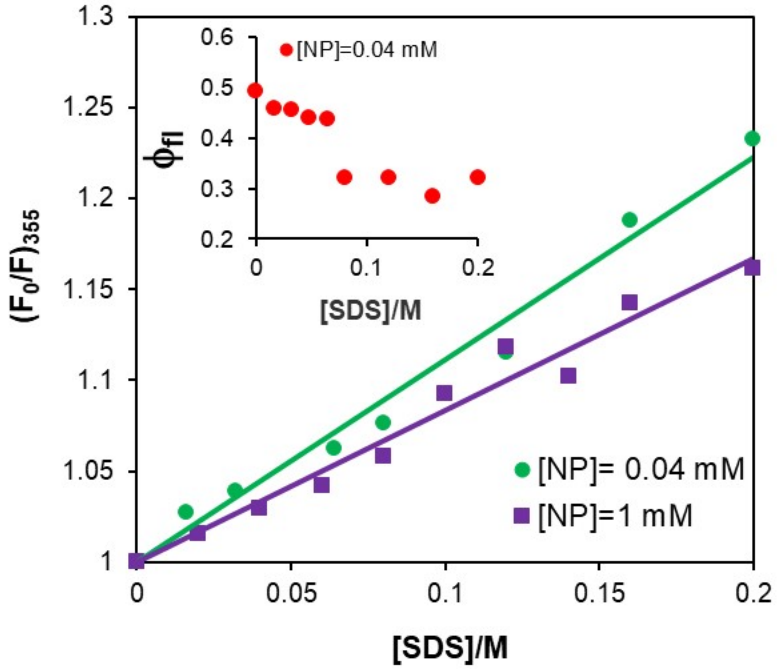

Figure 1: Plot of the ratio of NP fluorescence intensity in water, F_0, and that in the presence of different SDS concentrations (all of them above cmc) at emission wavelength λ_{em}=355 nm, at 20ºC. *Inset*: the plot of NP (0.04 mM) fluorescence quantum yield, ϕ_{fl}, vs SDS concentration.

The NP fluorescence quantum yield, ϕ_{fl}, (Figure 1, *Inset*), decreases with SDS concentration increase above cmc, from ϕ_{fl} = 0.49 in H_2O (in agreement with the reported value 0.41 [28]) to ϕ_{fl} =0.33 in 0.2M SDS aqueous solution. Therefore, the contribution of the radiationless decay of NP first singlet excited state, ^{1}NP, increases in the SDS micelle. This result is somewhat unexpected one since the micellar environment seems to afford a more rigid medium than water, restricting the vibrational freedom in ^{1}NP. Thus, one can suppose that some other deactivation pathways is active which overcome the vibrational relaxation effect. The more compact medium afforded by the micelle in comparison with water could promote the intersystem crossing of the drug, in fact phosphorescence of NP was observed in SDS [41]. On the other hand, hydrogen bonds formation in protic solvents and some aprotic media are reported to produce quenching of NP fluorescence [28]. The hydrogen bond formation could be promoted by charge repulsion near the micellar surface.

Some irregularity in the quenching behavior is observed around 0.08 M of SDS, more clearly reflected by ϕ_{fl} (Figure 1, *Inset*), indicating some change in the micellar structure. A similar behavior was previously observed at similar SDS concentrations in the spectroscopic properties of morin [42] and NB [17]. It was associated with the micelle growth and some variation of the shape of the micelle (see section *3.1.3*).

3.1.2. Naproxen Solubility in Aqueous Micellar SDS Solutions

The distribution of molecular forms of the drugs in octanol/water is a property usually included in databases, whereas the value for the ionized forms is less available. In addition, these data could not reproduce the distribution in other micro-heterogeneous media e.g. in micellar solutions.

Several methods have been described to determine the distribution of the drugs in micellar solution [43]. Most of them involve the determination of the solubility of the drug in the aggregates. This parameter is easy to measure experimentally for the poorly soluble in water molecules, but it is difficult for highly soluble ones.

For these reasons, partition of NP in SDS micellar solution was estimated from the drug solubility in H_2O at increasing SDS concentrations over a range of pH at 20ºC by uv-vis absorption spectroscopy [44]. This method allows partition determination of both, molecular and ionized NP, without the experimental determination of the ionized NP solubility. The solubility of the neutral drug is measured at different pHs where a mixture composition of both forms is known.

NP solubility linearly increases with SDS concentration at all pHs (S3) following the increase in the micelles concentration. Similar trend was observed in cationic, anionic or mixed cationic/non-ionic [45] or anionic/non-ionic [46] micelles.

As described in [44], the slope of the corresponding linear plots of the drug solubility in SDS solution related to that in water S_0^{SDS}/S_0^{H2O} vs. SDS volume fraction (Figure 2A) corresponds to NP partition coefficient P (S4) between the micellar and water phases.

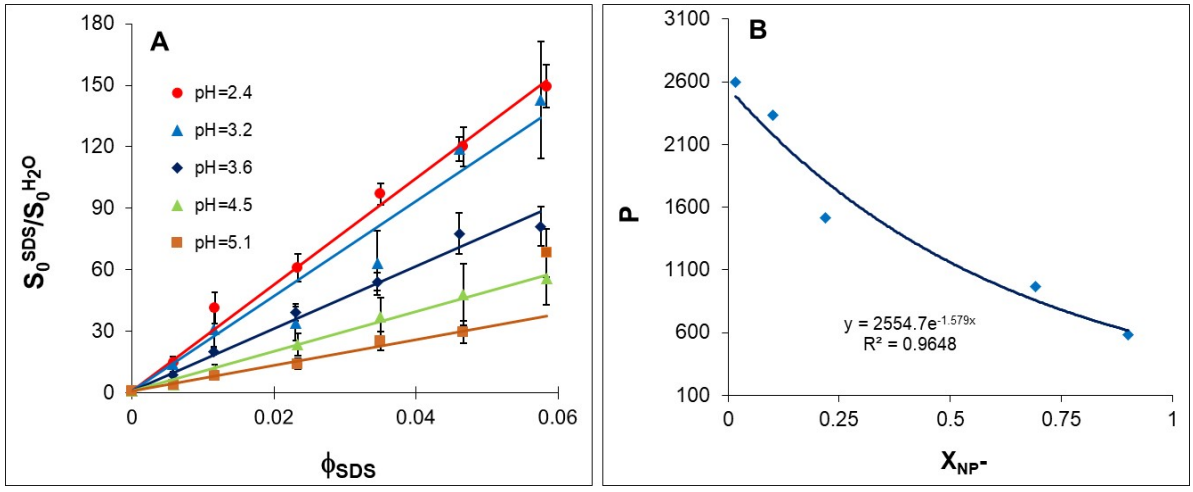

Figure 2: **A:** The plot of the ratio of NP solubility in SDS and in water vs. SDS volume fraction, ϕ_{SDS}, at different pHs; **B:** plot of the slope of the curves in A (partition coefficient, P, (S4)) vs. NP ionization degree X_{NP^-}. At 20ºC.

As can be observed (Figure 2A), the slope of the plots, and therefore, the value of P increases with pH decrease. At low pH the ionization equilibrium shifts towards the molecular nonionized form of the drug, which clearly partitions better in the micelle. This result confirms that the disappearance of the negative charge from the drug increases its partition in SDS as previously suggested [45]. The repulsions between the charged drug and the micellar surface is the reason for the lower partition of anionic NP in anionic micelles compared to cationic or non ionic ones [45] and the anionic/non-ionic mixtures [46]. Therefore, electrostatic effects play the important role in the affinity of the drugs for the micelles.

In contrast to the previously described behavior [44], the plot of the value of P at each pH (slope of the curves included in Figure 2A) vs. NP ionization degree is not linear (Figure 2B). Exponential fitting of the data and further extrapolation to 100% and 0% of ionization degree gives a partition coefficient of the ionized, P_{NP^-}=524 (logP=2.7), and the neutral, P_{NP}=2540 (logP=3.4), forms of NP. The partition coefficient value obtained for the neutral form of NP in SDS aqueous solution is in agreement with those reported for octanol/water, logP=3.3 [47] and log P = 3.18 [48]. By contrast, a significantly larger P value for ionized NP in SDS solution than that for octanol/water, log P= 0.32, was obtained [49]. The presence of water in the micelle could improve the solubilization of charged drugs. In fact, the larger number of ionized NP than that of the neutral one was found in lipid membranes [15]. Overall, partition coefficient values show that despite molecular form is partitioned better, the ionized NP also strongly tends to accumulate in the micellar domain and therefore it would do this in hydrophobic biological environments.

Interestingly, this result suggests that partitioning could contribute to the accumulation of NP in the intestinal cells like in the stomach cells, and not only NP can be ion-trapped within the enteric cells as reported [50].

Once confirmed that NP in ionized form is mainly located in the micellar phase, next we studied the effect of the presence of the negatively charged NP on the micelle structure by SANS.

3.1.3. Small-Angle Neutron Scattering, SANS, Study of SDS Aggregates

SANS curves of SDS aggregates formed at 50 and 200 mM surfactant concentration in the presence of 1mM NP (Figure 3) were obtained in order to check whether the NP loaded micelle shape or size are changing with SDS concentration. These concentrations are well bellow and above that where the change in the fluorescence quantum yield of the drug was observed (Figure 1, *Inset*).

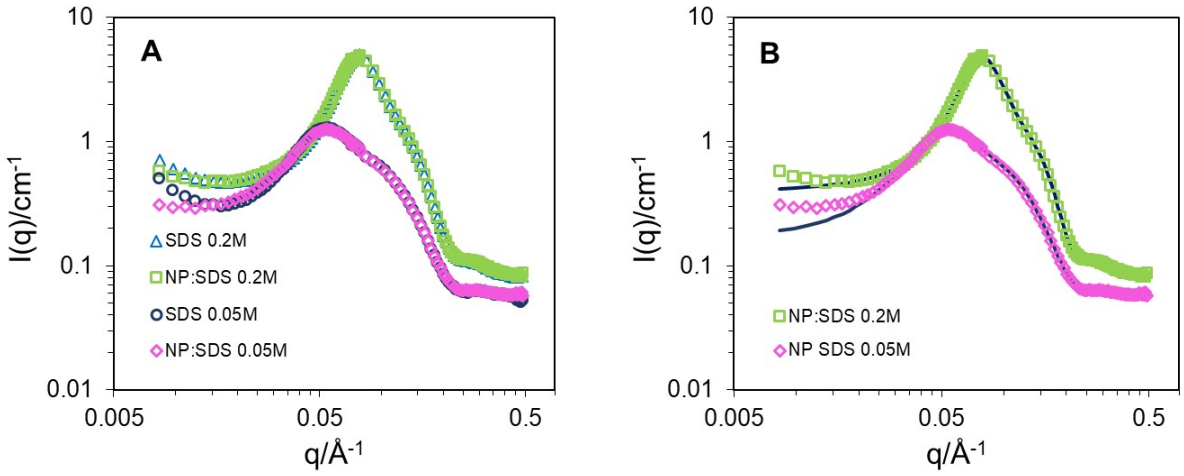

Figure 3: Small-angle neutron scattering data of SDS micelles free (circles and triangles) and loaded with 1 mM NP (diamonds and squares), at 0.05 M (○,◊) and 0.2 M (Δ, □) of SDS concentration, in D_2O at 25 ºC. **A:** free and loaded micelles curves at both SDS concentrations. **B:** NP curves as in A, but with the fits (solid lines) to the ellipsoidal micelle model [31,32].

As can be seen, (Figure 3), the curves for NP loaded SDS micelle nearly overlap those for micelles without NP, except at low q where the upturn in the scattering intensity is softened by the presence of the drug. This effect is more pronounced for micelles with larger amount of NP molecules (compare curves for 50 and 200 mM SDS concentration in the presence and in the absence of 1mM NP in Figure 3). The upturn at low q is related to the attractive depletion interactions in systems with coexistence of rods and spheres [51,52]. The upturn magnitude was taken as a measure of the extent of mixture of structures in SDS micelles [53]. Therefore, the presence of the charged NP seems to stabilize one type of micelle over the other, decreasing the depletion forces. This effect for NP is smaller than that for the neutral NB [17].

At both SDS concentrations, SANS curves of NP loaded aggregates are well fitted to an ellipsoidal micelles model (Figure 3B), similar to the case of free micelles [17,54]. The fitting parameters (Table 1) were compared to those for the free micelle previously reported [17]. The average amount of NP molecules per one micelle, estimated from Nagg (Table 1), equals to 1 and 0.25 at 0.05 and 0.2M of SDS, respectively.

System	Polar Radius/Å	Equatorial Radius/Å	Charge/e	Volume fraction	Nagg
SDS dil*	14.29 ± 0.039	22.31 ± 0.027	16.79 ± 0.068	0.0125	46
NP: SDS dil	14.28 ± 0.040	22.34 ± 0.028	14.63 ± 0.057	0.0123	47
SDS conc*	15.04 ± 0.011	23.14 ± 0.011	53.61 ± 0.540	0.0484	55

NP: SDS conc	15.05 ± 0.011	23.04 ± 0.039	46.78 ± 0.315	0.0485	54

Table 1: Parameters of fitting to ellipsoid micelles model of SANS curves for SDS solutions in D_2O, at 298 K, with 1mM NP (rows 2 and 4) and without NP (rows 1 and 3) (*data taken from ref. [17]). Concentration of SDS was *0.05M* (files1 and 2) and *0.2M* (files 3 and 4).

As can be observed (Table 1) the micelles grow with surfactant concentration. The presence of charged NP has no effect on the size, shape and aggregation number of the SDS micelle. Although, the micelle growth with SDS concentration could promote the non radiative transitions in ^1S, as suggested in the previous section, giving rise to the quenching of NP fluorescence observed (see section *3.1.3.*).

The NP presence in SDS solution results in a slightly lower surface charge of the micelle at both surfactant concentrations (Table 1). This indicates a decrease in the ionization degree of the aggregate with the presence of the charged drug and points to NP location in the vicinity of the micelle surface. The electrostatic repulsion between the drug and the negative micelle surface could also promote the intermolecular hydrogen bond formation of NP with water contributing to the observed quenching of fluorescence of the drug in the SDS micelle, as it was also speculated in the previous section.

3.2. Photodegradation of Naproxen in Aqueous Micellar SDS Solutions

The photodegradation of NP (1mM) in water and in the presence of 0.2M SDS was studied.

Irradiation of NP in water and in SDS micellar solution with light of 313 nm initially leads to a decrease in intensity of the NP band at λ_{em} =355 nm (F_{355}) showing the drug photodegradation and to the concurrent increase of the intensity of a new band of some product at λ_{em} =440 nm (F_{440}) (Figure 4).

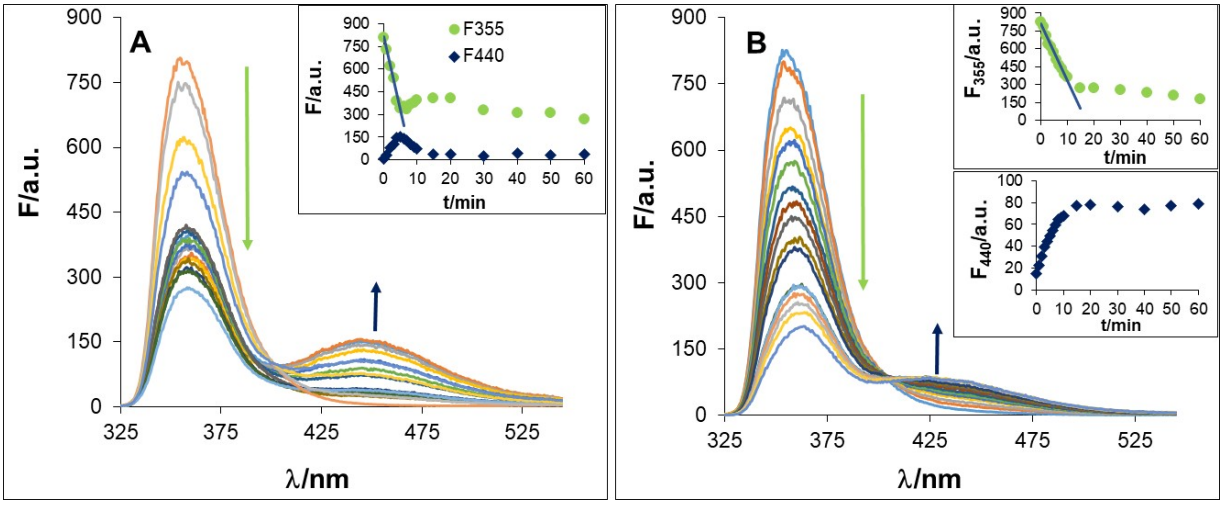

Figure 4: Fluorescence spectra of 1 mM NP at different irradiation times in: **A:** water, and **B:** 0.2M SDS. *Insets*: plots of the intensity of the bands corresponding to NP at λ_{em}=355 nm (F_{355}) and the photoproduct at λ_{em}=440 nm (F_{440}) vs. the irradiation time. The black lines correspond to the fittings of the data to a zero order kinetic. The spectra were obtained with λ_{exc}= 317 nm.

Initial NP photodegradation follows a zero order kinetic in both media, as previously reported [12,13]. The rate constant values were determined from the fitting of the slope of the plot of F_{355} vs. irradiation time, (Figure 4A and 4B, *Insets*), corrected by the fluorescence-concentration proportionality constant of NP, obtained at each set from the ratio of fluorescence intensity and drug concentration before irradiation, F_0/C_0. The zero order rate constant values of k_{PD} = (1.29 ± 0.38) 10^{-6}, and k_{PD} = (1.21 ± 0.22) 10^{-6} M s^{-1}, were obtained for the NP photodegradation in water and SDS micelle, respectively. The photodegradation quantum yield, $\phi_{PD,}$ calculated from k_{PD} were ϕ_{PD} = (4.21 ± 1.22) x 10^{-2} and (3.94 ± 0.70) x 10^{-2} for NP in H_2O and SDS, respectively. These results show that encapsulation in SDS micelle does not protect the drug against light at the initial stage of photolysis. No data in other micellar media have been found in the literature. But, this behavior seems to be different to that described in other heterogeneous media. For instance, inclusion complex formation of NP with hydroxypropyl-β-CD (HP-β-CD) protects the drug against light [13]; whereas, that with β-CD does not [12], or even increases NP photodegradation [11], depending on the technique used. Therefore, the reactivity of the drug triggered by light is highly dependent on the environment. However, this relationship is not very clear (see below).

Further irradiation of NP in water results in the disappearance of the product fluorescence at λ_{em}=440 nm, while the intensity in the fluorescence region of NP, $F_{355,}$ even increases, followed by a slow decline at long irradiation times (insert in Figure 4A). Such behavior suggests the photodegradation of the photoproduct with λ_{em}=440 nm. However, this photoproduct seems to be relatively photostable in SDS solutions (insert in Figure 4B).

NP photodegradation is known to form several photoproducts [5]. The photoproducts most frequently found are (Scheme 1): 6-methoxy-2-(1-hydroxyethyl)-naphthalene, **(2)**, and 6-methoxy-2-acetyl-naphthalene, **(3)**. The absorption spectrum of **(2)** overlaps to that of the undegraded drug **(1)**, and it is expected to emit at the same wavelength [11,12], whereas **(3)** shows an absorption maximum at 312 nm [11] and it emits at 440 nm [12].

NP photodegradation quantum yield obtained from fluorescence could be underestimated depending on the amount of **(2)** formed in each medium, as pointed out in the case of β-CD [11,12]. In fact, ϕ_{PD} =0.11 was obtained for NP in water [12].

Fluorescence is a very useful tool to detect photodegradation and formation of small amounts of fluorescent compounds. However, it is not able to accurately quantify the photodegradation degree if the signals of the drug and photoproducts overlap, as it was previously pointed out for absorption spectroscopy [11]

Therefore, further experiments are required in order to confirm the effect of NP encapsulation in SDS micelle on NP photoreactivity and to check the nature of the photoproducts formed in both media.

3.2.1. Gases Chromatography/ Mass Spectrometry (GC/MS) Photoproducts Determination

Naproxen 1mM samples irradiated at 1, 2, 25 min in H_2O, and at 2, 3, 25 min in 0.2M SDS, were analyzed by GC/MS. At all irradiation times, two photoproducts namely, 6-methoxy-2 (1-hydroxyethyl) naphthalene, **(2)**, and 6-methoxy-2-acetyl-naphthalene **(3)** (Scheme 1), were found. These compounds appeared in a great majority of the media studied [5–8,11,12].

The peaks of both photoproducts presented higher counts in water (S5) than in SDS (S6) at all the irradiation times checked. This finding demonstrated undoubtedly, that NP encapsulation in the restricted SDS micellar environment protects the drug against photodegradation. The formation of the alcoholic derivative **(2)** in higher amount in water than in SDS, confirms the larger photodegradation quantum yield in water than that obtained by fluorescence, due to the overlapping of this photoproduct and the undegraded NP emission spectrum [11,12]. The toxicity of **(2)** over the hepatic cells is the highest of all the possible photoproducts formed by the drug irradiation, but it is dangerous only in large amounts [55]. Thus, toxicity mediated by the final photoproducts is expected to decrease in the restricted medium of the SDS micelle.

The analysis of the evolution of the peaks of both photoproducts with the irradiation time shows that the signal from **(3)** (the aldehyde photoproduct) increases with the irradiation time in both media (S5 and S6). By contrast, different behavior of the alcoholic photoproduct **(2)** is observed when NP is irradiated in SDS micelle with respect to that in water. In water, the highest amount of **(2)** (S5) appears at very short irradiation time; and it disappears as the irradiation time increases. This trend clearly shows that the alcoholic photoproduct **(2)** suffers quick secondary photodegradation in aqueous medium. However, when NP is irradiated in SDS, MS peak of **(2)** (S6) increases continuously with irradiation time (from 2, 3 to 25 min), even at higher irradiation times (data not shown). Nonetheless its concentration remains always much lower than that in water at any time. This behavior demonstrates that SDS micelle strongly avoids the alcoholic photoproduct **(2)** formation.

The percentage of **(3)** in the photomixture increases: 1.3, 1.2, 5.4 % with irradiation time (1, 2, 25 min) in H_2O, and 3.3, 3.5, to 15.7 % (2, 3, 25 min) in SDS. So, **(2)** is the main component in both media; this result is in good agreement to the previous studies in SDS [11]. However, **(3)** was reported as the main component of the phtotomixture in water [14], but in this case the sample was analyzed after 4h of irradiation. This difference observed in photomixture composition in water is in good agreement to the disappearance of the alcoholic photoproduct with the irradiation time.

The photomixture composition at different irradiation times shows the oxidized compound (3) appears faster in SDS than in H_2O. This photoproduct (3) can be formed by two different pathways [5]: (i) via NP radical cation after it's decarboxylation in the presence of O_2; or (ii) via the benzylic radical transformed to (2) in the presence of O_2 followed by the oxidation or

456 photooxidation of the alcohol (2) (S7). SDS has been recently reported to prevent efficiently
457 the oxidation of NB [17], NSAID structurally related to NP but without acidic nature. Since,
458 NP radical cation is formed in biphotonic process then the mechanism (i) seems to be not very
459 important under the natural conditions (see next section).

460

461 *3.2.2. Intermediates of Photolysis of NP in Aqueous Micellar SDS Solutions*

462 In laser flash photolysis experiments, SDS concentration was 0.2 M and that of NP in the
463 range 0.5 - 3 mM. These concentrations were selected in order to get enough absorption of NP
464 at 337 nm (N_2-laser wavelength), and to keep condition that amount of NP molecule per
465 micelle is less than 1. At this conditions there is practically no effects related to the interaction
466 of two or more NP molecules within a given micelle.

467 The nanosecond laser flash photoexcitation of NP in neutral aqueous SDS solution (where NP
468 seems to be in ionized form NP^-) results in the formation of at least three intermediates
469 observed immediately after the laser pulse (Figure 5, curve 1). They are characterized by
470 transient absorption with maxima at 440 and 720 nm with shoulder near 620 nm and by
471 significantly different lifetimes (16 μs, 0.08 and 1 μs, respectively). The proposed kinetic
472 scheme of the primary photoprocesses of NP in SDS aqueous solutions are included in S8.
473
474

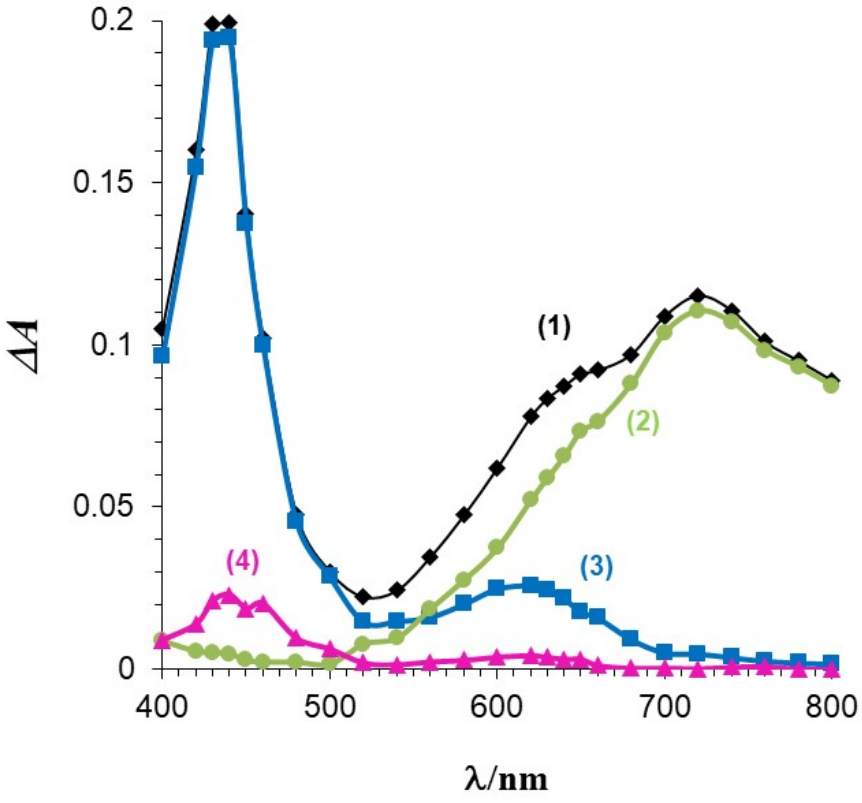

475
476 **Figure 5:** UV-vis transient absorption spectra of intermediates obtained upon laser flash
477 photolysis of aerated aqueous solutions of NP (1 mM) in the presence of SDS (0.2 M) in 0.02

(1), 0.25 **(3)** and 15 **(4)**, μs after the laser pulse and **(2)** is the difference of absorption spectra (1) and (3) representing the absorption spectra of e_{aq}.

The relatively narrow band with characteristic maximum at 440 nm can be assigned to the triplet excited state (^{3}NP) [7,9]. The broad absorption with maximum around 720 nm and short lifetime is the well known characteristic of the hydrated electron e_{aq}^{SDS} as it was previously observed in homogeneous water solutions [7,9]. The shoulder near 620 nm seems to be due to the contribution of naproxen neutral radical (NP$^{\bullet}$) or as previously reported to radical cation ($NP^{+\bullet}$) [9].

The e_{aq}^{SDS} absorption spectrum (Figure 5, curve 2) calculated by subtraction of the initial transient absorption (Figure 5, curve 1) and the residual transient absorption observed after e_{aq}^{SDS} decay (Figure 5, curve 3) is very similar to that in pure water [56]. It is reasonable to expect that e_{aq}^{SDS} is localized in a water phase since e_{aq}^{SDS} escapes from the micelle to the water bulk due to the electrostatic repulsion from the negatively charged micelle.

The dependence of e_{aq}^{SDS} yield on the laser energy was quadratic in SDS solutions as well as it was found earlier in homogeneous media [9]. Therefore, the NP photoionization is a biphotonic process. The e_{aq}^{SDS} decay kinetics is monoexponential with first order rate constant (k_e) near $1.3*10^7$ s^{-1} in deaerated SDS solutions. This value is more than two and one orders of magnitude larger than that observed in pure water ($\leq 1*10^5$ s^{-1} [56]) and in the case of SDS aqueous solutions of the related compound NB [17]. It was speculated that the fast decay of e_{aq}^{SDS} in SDS solutions of NB was due to the quenching of e_{aq}^{SDS} by the residual amount of NB in the water phase. The amount of residual ionized NP in the water phase is significantly larger than that of NB, which results in significantly faster decay of e_{aq}^{SDS} in spite of the negative charge of ionized NP.

The decay of e_{aq}^{SDS} becomes noticeably faster under the aerated conditions. The value of the rate constant of e_{aq}^{SDS} quenching by molecular oxygen equal to $1.5*10^{10}$ $M^{-1}s^{-1}$ was estimated using the oxygen concentration of 0.28 mM [57] in air saturated water. It is well known that the quenching of e_{aq}^{SDS} by molecular oxygen is controlled by diffusion. The formation of reactive radical $O_2^{-\bullet}$ is expected, but with the yield not more than 20% due to the very short lifetime of e_{aq}^{SDS}. In the case of NB in SDS solutions the life-time of e_{aq}^{SDS} was long enough for the complete quenching of e_{aq}^{SDS} by O_2 in aerated solutions and the expected yield of $O_2^{-\bullet}$ was close to 100% [17]. Therefore, in this regard the photosensitization effect of NP is five times smaller than that of NB.

The ^{3}NP and NP radical absorption with maxima at 440 and 620 nm, respectively, were observed after the complete decay of e_{aq}^{SDS} (Figure 5, curve 3).

The decay kinetics of NP radical observed in SDS solution was the first order with rate constant near $1x10^6$ s^{-1} and it was independent on the presence of air. This value is similar to that observed for the decay of NP radical cation in homogeneous aqueous solution [9] but clearly smaller than e_{aq}^{SDS} decay.

The decay kinetics of NP radical in SDS solution was independent on [NP]. Thus, a dimer formation between NP radical and NP is not important under the experimental conditions used

519 in the present work. This observation is in contrast to that for radical cations of naphthalene
520 and some derivatives which reacts with their ground state to form radical cation of dimer at
521 large enough concentration of naphthalene [58,59]. In spite of the fact that electron donating
522 substituents in naphthalene moiety favors the dimer cation formation, in the case of NP in
523 SDS solution, the micelle prevents the bimolecular reaction of NP radical in one micelle with
524 NP in the other. Although-minor amounts of dimers could be formed in reaction of NP radical
525 with residual NP in water phase or in small amount of micelles with a couple of NP
526 molecules. However, based on previous calculations (Section *3.1.3.*), the amount of micelles
527 with more than two NP molecules is practically negligible for the solutions with
528 concentrations of SDS and NP used.

529 The absorption of NP radical was compared to that of e_{aq}^{SDS} (see Fig. 5, spectra 2 and 3). It is
530 reasonable to suppose that e_{aq}^{SDS} and NP radical are formed in equal amount. The value $\varepsilon =$
531 $3*10^3$ $M^{-1}cm^{-1}$ for NP radical at 620 nm was estimated using e_{aq}^{SDS} extinction coefficient equal
532 to that in water ($1.85*10^4$ $M^{-1}cm^{-1}$ [56]). This value is significantly smaller than that for NB
533 radical cation in SDS solution [17], which is not expected on the bases of their similar
534 structure. This behavior suggests that the amount of radical with this slow decay is smaller
535 than the total amount of radicals formed. Thus, one can suppose that the most part of NP
536 radicals initially formed decays with the rate constant comparable with or even faster than that
537 of e_{aq}^{SDS} decay. The fast decay part of NP radical was difficult to extract quantitatively
538 because of the NP radical absorption overlaps with that of e_{aq}^{SDS}.

539 The rate of the slow decay of NP radical in SDS solution is of the same order than that in
540 homogeneous media, where decarboxylation was demonstrated to be the main pathway for the
541 NP radical deactivation [5].

542 The biphotonic photoionization of NP seems to play an insignificant role in normal conditions
543 since it needs the large power light. So, in SDS the main photodegradation pathway seems to
544 be through the benzylic radical ($R^{\bullet}$ S7) and then the formation of (3) from (2) by oxidation,
545 demonstrating that the oxidation of (2) is promoted in SDS (see discussion in section *3.2.1.*),
546 by contrast to the behavior recently observed for NB [60]. In addition, the reaction of ^{3}NP
547 seems to be more important in the photoproduct formation.

548 The ^{3}NP decay kinetics in deaerated SDS solution is monoexponential with first order rate
549 k=$6.2•10^4$ s^{-1}. Although, this value is of the same order of magnitude as those reported for ^{3}NP
550 decay in homogeneous media [7,9]; however by contrast to the homogeneous media, the
551 triplet-triplet annihilation of ^{3}NP was not observed in SDS solution, due to the small diffusion
552 coefficient and screening of ^{3}NP localized in micellar phase.

553 The decay of ^{3}NP accelerates significantly in the presence of molecular oxygen in SDS
554 solution. The value of quenching rate constant of ^{3}NP by O_2 equal to $1.8*10^9$ $M^{-1}s^{-1}$ was
555 calculated using the oxygen concentration in air saturated water 0.28 mM [57]. The quenching
556 of ^{3}NP by O_2 occurs by triplet-triplet energy transfer, which is the diffusion-controlled process
557 with spin-statistical factor 1/9. The formation of reactive singlet oxygen $^1O_2$ was detected in
558 homogeneous media [61] as well as in SDS [7].

One other relatively long-lived transient absorption near 450 nm remained even after the decay of the ^{3}NP was complete (Figure 5, curve 4). The decay kinetics of this transient is first order with rate constant k=1.5•10^4 s^{-1}. A transient with very similar absorption spectra was observed recently in water-acetonitrile mixture and assigned to the decarboxylated radical of ionized NP formed from the triplet state of ionized NP [10] that can be assigned to the benzylic one (R$^\bullet$ S7). The lifetime of that radical in water-acetonitrile mixture was near 700 ns, which is two orders of magnitude shorter than the lifetime of similar transient observed in the present work in aqueous SDS solution. One can conclude that SDS micelles offer a stabilization effect on the precursors of the final products of NP photolysis. This result is in good agreement to the alcoholic photoproduct formation as limiting step of the drug photodegradation. The propossed mechanism is included in S7.

The stabilization could be related to the subtraction of the hydrogen needed to form the photoproduct from SDS as demonstrated in β-CD inclusion complex [11]. By contrast, to the β-CD, SDS seems to be less readily to donate a hydrogen atom than the homogeneous media.

Overall, the behavior of transient photoproducts of NP in aqueous SDS solution has the specific features if to compare with that in homogeneous environment. On one hand, the formation of active form of oxygen is still efficient and thus NP could be a potential photosensitizer contributing to the overall phototoxicity. However, it is interestingly that SDS micelles stabilize the precursors of the final products of NP photolysis.

Conclusions

The photochemistry of widespread anti-inflammatory drug naproxen in anionic form in aqueous solutions of anionic micelles SDS was investigated for the first time. Several techniques were used in order to reveal basic features of the NP photochemistry in micellar environment. The nature and kinetics of the relatively stable final and short lived intermediate photoproducts were obtained.

It was shown that despite neutral molecular form of NP partitions better in micellar phase, the anionic one also highly partitions in anionic SDS micelles. Partition of the drug into the micellar phase promotes the quenching of NP fluorescence, but it has soft impact on the micelle features.

SDS micelles protect anionic NP from the photodegradation. The process of NP photodegradation includes the formation of the triplet excited state. One of the secondary but supposed the key reaction of the triplet state results in the reduction with formation of radicals which are stabilized by micelles. This radical screening seems to be responsible for NP$^-$ protection from the light by SDS micelles.

The specific protective effect on the photodegradation of NP in the SDS micelle was found. SDS micelles significantly avoids the alcoholic photoproduct **(2)** formation which is formed at the initial stage of the NP photodegradation. Whereas the oxidation of the alcoholic photoproduct **(2)** is faster in SDS than in water.

From a practical point of view, the results suggest the possibility of bioaccumulation of the drug in hydrophobic parts of biological structures. The lower photoreactivity in the micelles than in water is a hopeful result from toxicological point of view, but on the other hand it would increase the persistence of the pharmaceutical in the natural environment.

Acknowledgement

This work is based upon experiments performed at the KWS-2 instrument operated by JCNS at the Heinz Maier-Leibnitz Zentrum (MLZ), Garching, Germany. This work benefited from the use of the Sas- View application, originally developed under NSF Award DMR- 0520547. SasView also contains code developed with funding from the EU Horizon 2020 programme under the SINE2020 project. Grant No 654000.

References

[1] The Top 300 of 2020, ClinCalc. (n.d.).
[2] Naproxen - Drug Usage Statistics, ClinCalc. (n.d.).
[3] A.J. Ebele, M. Abou-Elwafa Abdallah, S. Harrad, Pharmaceuticals and personal care products (PPCPs) in the freshwater aquatic environment, Emerg. Contam. 3 (2017) 1–16. https://doi.org/10.1016/j.emcon.2016.12.004.
[4] S.L. Klosterhaus, R. Grace, M.C. Hamilton, D. Yee, Method validation and reconnaissance of pharmaceuticals, personal care products, and alkylphenols in surface waters, sediments, and mussels in an urban estuary, Environ. Int. 54 (2013) 92–99. https://doi.org/http://dx.doi.org/10.1016/j.envint.2013.01.009.
[5] F. Boscá, M.L. Marín, M.A. Miranda, Photoreactivity of the Nonsteroidal Anti-inflammatory 2-Arylpropionic Acids with Photosensitizing Side Effects¶, Photochem. Photobiol. 74 (2001) 637–651. https://doi.org/10.1562/0031-8655(2001)074<0637:potnai>2.0.co;2.
[6] D.E. Moore, Mechanisms of photosensitization by phototoxic drugs, Mutat. Res. - Fundam. Mol. Mech. Mutagen. 422 (1998) 165–173. https://doi.org/10.1016/S0027-5107(98)00189-4.
[7] D.E. Moore, P.P. Chappuis, A comparative study of the photochemistry of the non-steroidal anti-inflammatory drugs, naproxen, benoxaprofen and indomethacin and indomethacin, Photochem. Photobiol. 47 (1988) 173–180. https://doi.org/10.1111/j.1751-1097.1988.tb02710.x.
[8] F. Boscá, M.A. Miranda, L. Vañó, F. Vargas, New photodegradation pathways for Naproxen, a phototoxic non-steroidal anti-inflammatory drug, J. Photochem. Photobiol. A Chem. 54 (1990) 131–134. https://doi.org/10.1016/1010-6030(90)87018-7.
[9] L.J. Martínez, J.C. Scaiano, Characterization of the Transient Intermediates Generated from the Photoexcitation of Nabumetone: A Comparison with Naproxen, Photochem. Photobiol. 68 (1998) 646–651. https://doi.org/10.1111/j.1751-1097.1998.tb02524.x.
[10] R. Liang, S.S. Sun, G. Huang, M. De Li, Unveiling the Photophysical and Photochemical Reaction Process of Naproxen via Ultrafast Femtosecond to Nanosecond Laser Flash Photolysis, Chem. Res. Toxicol. 32 (2019) 613–620.

https://doi.org/10.1021/acs.chemrestox.8b00310.
[11] M.C. Jiménez, M.A. Miranda, R. Tormos, Photochemistry of naproxen in the presence of β-cyclodextrin, J. Photochem. Photobiol. A Chem. 104 (1997) 119–121. https://doi.org/10.1016/s1010-6030(97)00013-0.
[12] M. Valero, C. Carrillo, Effect of binary and ternary polyethyleneglycol and/or β-cyclodextrin complexes on the photochemical and photosensitizing properties of Naproxen, J. Photochem. Photobiol. B Biol. 74 (2004) 151–160. https://doi.org/10.1016/j.jphotobiol.2004.03.004.
[13] M. Valero, B. Esteban, Effect of binary and ternary polyvinylpyrrolidone and/or hydroxypropyl-β-cyclodextrin complexes on the photochemical and photosensitizing properties of Naproxen, J. Photochem. Photobiol. B Biol. 76 (2004) 95–102. https://doi.org/10.1016/j.jphotobiol.2004.06.005.
[14] J. V. Castell, M.J. Gomez-Lechon, C. Grassa, L.A. Martinez, M.A. Miranda, P. Tarrega, Involvement of drug-derived peroxides in the phototoxicity of naproxen and tiaprofenic acid, Photochem. Photobiol. 57 (1993) 486–490. https://doi.org/10.1111/j.1751-1097.1993.tb02323.x.
[15] A. Yousefpour, S. Amjad Iranagh, Y. Nademi, H. Modarress, Molecular dynamics simulation of nonsteroidal antiinflammatory drugs, naproxen and relafen, in a lipid bilayer membrane, Int. J. Quantum Chem. 113 (2013) 1919–1930. https://doi.org/10.1002/qua.24415.
[16] D.S. Pellosi, B.M. Estevão, J. Semensato, D. Severino, M.S. Baptista, M.J. Politi, N. Hioka, W. Caetano, Photophysical properties and interactions of xanthene dyes in aqueous micelles, J. Photochem. Photobiol. A Chem. 247 (2012) 8–15. https://doi.org/10.1016/j.jphotochem.2012.07.009.
[17] M. Valero, P.P. Levin, N.B. Sultimova, J.E. Houston, Photochemistry of nabumetone in aqueous solution of sodium dodecylsulfate (SDS) micelles, J. Mol. Liq. 00 (2020) 00.
[18] S. Sortino, L.J. Martínez, G. Marconi, On the photophysical and photochemical behavior of fenbufen: A study in homogeneous media and micellar environments, New J. Chem. 25 (2001) 975–980. https://doi.org/10.1039/b100164g.
[19] P. Opanasopit, T. Ngawhirunpat, T. Rojanarata, C. Choochottiros, S. Chirachanchai, N-Phthaloylchitosan-g-mPEG design for all-trans retinoic acid-loaded polymeric micelles, Eur. J. Pharm. Sci. 30 (2007) 424–431. https://doi.org/10.1016/j.ejps.2007.01.002.
[20] K. Huang, G. Lu, Z. Zheng, R. Wang, T. Tang, X. Tao, R. Cai, Z. Dang, P. Wu, H. Yin, Photodegradation of 2,4,4′-tribrominated diphenyl ether in various surfactant solutions: Kinetics, mechanisms and intermediates, Environ. Sci. Process. Impacts. 20 (2018) 806–812. https://doi.org/10.1039/c8em00033f.
[21] C. Lu, X. Yin, X. Liu, M. Wang, Study of the photodegradation kinetics and pathways of Hexaflumuron in liquid media, Photochem. Photobiol. 90 (2014) 1219–1223. https://doi.org/10.1111/php.12314.
[22] K. Jardak, P. Drogui, R. Daghrir, Surfactants in aquatic and terrestrial environment: occurrence, behavior, and treatment processes, Environ. Sci. Pollut. Res. 23 (2016) 3195–3216. https://doi.org/10.1007/s11356-015-5803-x.
[23] M. Valero, L.J. Rodriguez, M.M. Velazquez, Inclusion of non-steroidal anti-inflammatory agents into aqueous cyclodextrins: A UV-absorption spectroscopic study, Farmaco. 51 (1996) 525–533.
[24] M. Valero, S.M.B. Costa, Photodegradation of Nabumetone in aqueous solutions, J.

689 Photochem. Photobiol. A Chem. 157 (2003) 93–101. https://doi.org/10.1016/S1010-
690 6030(03)00013-3.
691 [25] M. Valero, Photodegradation of Nabumetone in n-butanol solutions, J. Photochem.
692 Photobiol. A Chem. 163 (2004) 159–164.
693 https://doi.org/10.1016/j.jphotochem.2003.11.005.
694 [26] https://pubchem.ncbi.nlm.nih.gov/compound/Naproxen (accessed May 20, 2020).
695 [27] B.L. Bales, A definition of the degree of ionization of a micelle based on its
696 aggregation number, J. Phys. Chem. B. 105 (2001) 6798–6804.
697 https://doi.org/10.1021/jp004576m.
698 [28] M.M. Velazquez, M. Valero, L.J. Rodríguez, S.M.B. Costa, M.A. Santos, Hydrogen
699 bonding in a non-steroidal anti-inflammatory drug-Naproxen, J. Photochem. Photobiol.
700 B Biol. 29 (1995) 23–31. https://doi.org/10.1016/1011-1344(95)90245-7.
701 [29] A.N. Fletcher, Quinine sulfate as a fluorescence quantum yield standard, Photochem.
702 Photobiol. (1969) 221–224. https://doi.org/10.1111/j.1751-1097.1969.tb07311.x.
703 [30] A. Radulescu, N.K. Szekely, M.S. Appavou, V. Pipich, T. Kohnke, V. Ossovyi, S.
704 Staringer, G.J. Schneider, M. Amann, B. Zhang-Haagen, G. Brandl, M. Drochner, R.
705 Engels, R. Hanslik, G. Kemmerling, Studying soft-matter and biological systems over a
706 wide length-scale from nanometer and micrometer sizes at the small-angle neutron
707 diffractometer KWS-2, J. Vis. Exp. 2016 (2016) 1–23. https://doi.org/10.3791/54639.
708 [31] L.A. Feigin, D.I. Svergun, Structure Analysis by Small-Angle X-Ray and Neutron
709 Scattering, Plenum Press, new York, 1987.
710 [32] A. Isihara, Photoinduced phase separation in the lead halides is a polaronic effect, J.
711 Chem. Phys. 18 (1950) 1446–1449.
712 [33] C.G. Malmberg, Dielectric constant of deuterium oxide, J. Res. Natl. Bur. Stand.
713 (1934). 60 (1958) 609–612. https://doi.org/10.6028/jres.060.060.
714 [34] I. Grillo, I. Morfin, S. Prévost, Structural Characterization of Pluronic Micelles
715 Swollen with Perfume Molecules, Langmuir. 34 (2018) 13395–13408.
716 https://doi.org/10.1021/acs.langmuir.8b03050.
717 [35] H.H. Tönnensen, Photostability of Drugs and Drug Formulations, Second Edition, CRC
718 Press, Boca Raton, 2004. https://doi.org/10.1201/9781420023596.
719 [36] H. Heath, A new sensitive chemical actinometer - II. Potassium ferrioxalate as a
720 standard chemical actinometer, Proc. R. Soc. London. Ser. A. Math. Phys. Sci. 235
721 (1956) 518–536. https://doi.org/10.1098/rspa.1956.0102.
722 [37] G.W. Castellan, Physical Chemistry, 2nd ed., Addison Wesley S.A, México, 1987.
723 [38] T. Mill, W.R. Mabey, B.Y. Lan, A. Baraze, Photolysis of polycyclic aromatic
724 hydrocarbons in water, Chemosphere. 10 (1981) 1281–1290.
725 https://doi.org/10.1016/0045-6535(81)90045-X.
726 [39] P.P. Levin, N.B. Sul'timova, O.N. Chaikovskaya, Kinetics of fast reactions of triplet
727 states and radicals under photolysis of 4,4′-dimethylbenzophenone in the presence of 4-
728 halophenols in micellar solutions of sodium dodecyl sulfate in magnetic field, Russ.
729 Chem. Bull. 54 (2005) 1433–1438. https://doi.org/10.1007/s11172-005-0423-0.
730 [40] N.B. Sul'timova, P.P. Levin, O.N. Chaikovskaya, Laser photolysis study of the
731 transient products of 4-carboxybenzophenone-sensitized photolysis of
732 chlorophenoxyacetic acid-based herbicides in aqueous micellar solutions, High Energy
733 Chem. 44 (2010) 393–398. https://doi.org/10.1134/S0018143910050073.
734 [41] I.R. Martínez, R.M.V. Camañas, M.C. García-Alvarez-Coque, Micelle-stabilized room-
735 temperature phosphorimetric procedure for the determination of naproxen and

736 propranolol in pharmaceutical preparations, Analyst. 119 (1994) 1093–1097.
737 https://doi.org/10.1039/AN9941901093.
738 [42] W. Liu, R. Guo, Interaction between morin and sodium dodecyl sulfate (SDS) micelles,
739 J. Agric. Food Chem. 53 (2005) 2890–2896. https://doi.org/10.1021/jf047847p.
740 [43] N.C. Santos, M. Prieto, M.A.R.B. Castanho, Quantifying molecular partition into
741 model systems of biomembranes: An emphasis on optical spectroscopic methods,
742 Biochim. Biophys. Acta - Biomembr. 1612 (2003) 123–135.
743 https://doi.org/10.1016/S0005-2736(03)00112-3.
744 [44] J.H. Collett, R. Withington, Partition coefficients of salicylic acid between water and
745 the micelles of some non-ionic surfactants, J. Pharm. Pharmacol. 24 (1972) 211–214.
746 https://doi.org/10.1111/j.2042-7158.1972.tb08966.x.
747 [45] P.A. Bhat, G.M. Rather, A.A. Dar, Effect of surfactant mixing on partitioning of model
748 hydrophobic drug, Naproxen, between aqueous and micellar phases, J. Phys. Chem. B.
749 113 (2009) 997–1006. https://doi.org/10.1021/jp807229c.
750 [46] P.A. Bhat, O.A. Chat, A.A. Dar, Studies on binary mixtures of Pluronic P123 and twin
751 tailed 1-Butyl-3-methyl-imidazolium Aerosol OT - Aggregation behavior and impact
752 on Naproxen and Rifampicin partitioning, J. Mol. Liq. 241 (2017) 114–122.
753 https://doi.org/10.1016/j.molliq.2017.05.140.
754 [47] Computed Properties by XLogP3 3.0 (PubChem release 2019.06.18), (n.d.).
755 https://pubchem.ncbi.nlm.nih.gov/compound/156391 (accessed September 8, 2020).
756 [48] C. Hansch, A. Leo, D. Hoekman, Exploring QSAR - Hydrophobic, Electronic, and
757 Steric Constants, in: Explor. QSAR - Hydrophobic, Electron. Steric Constants,
758 American Chemical Society, Washington, DC, 1995: p. 121.
759 [49] ChemAxon, (n.d.). www.chemicalize.org (accessed June 2, 2014).
760 [50] P.D. Bryson, Nonsteroidal anti-inflammatory agents. In: Comprehensive review in
761 toxicology for emergency clinicians, 3rd ed., Washington, DC, 1996.
762 [51] X. Ye, T. Narayanan, P. Tong, J.S. Huang, Neutron scattering study of depletion
763 interactions in a colloid-polymer mixture, Phys. Rev. Lett. 76 (1996) 4640–4643.
764 https://doi.org/10.1103/PhysRevLett.76.4640.
765 [52] K.H. Lin, J.C. Crocker, A.C. Zeri, A.G. Yodh, Colloidal interactions in suspensions of
766 rods, Phys. Rev. Lett. 87 (2001) 88301-1-88301–4.
767 https://doi.org/10.1103/PhysRevLett.87.088301.
768 [53] P.A. Hassan, G. Fritz, E.W. Kaler, Small angle neutron scattering study of sodium
769 dodecyl sulfate micellar growth driven by addition of a hydrotropic salt, J. Colloid
770 Interface Sci. 257 (2003) 154–162. https://doi.org/10.1016/S0021-9797(02)00020-6.
771 [54] J.B. Hayter, A rescaled MSA structure factor fordiluted charged colloidal dispersions,
772 Mol. Phys. 46 (1982) 651–656.
773 [55] J. V. Castell, M.J. Gomez-Lechon, C. Grassa, L.A. Martinez, M.A. Miranda, P.
774 Tarrega, Involvement of drug-derived peroxides in the phototoxicity of naproxen and
775 tiaprofenic acid., Photochem. Photobiol. 57 (1993) 486–490.
776 https://doi.org/10.1111/j.1751-1097.1993.tb02323.x.
777 [56] M.A. Hart, The Hydrated Electron, John Wiley & Sons Original, 1970.
778 [57] R. Battino, T.R. Rettich, T. Tominaga, The Solubility of Oxygen and Ozone in Liquids,
779 J. Phys. Chem. Ref. Data. 12 (1983) 163–178. https://doi.org/10.1063/1.555680.
780 [58] S. Steenken, C.J. Warren, B.C. Gilbert, Generation of radical-cations from naphthalene
781 and some derivatives, both by photoionization and reaction with so4-˙: Formation and
782 reactions studied by laser flash photolysis, J. Chem. Soc. Perkin Trans. 2. (1990) 335–

342. https://doi.org/10.1039/p29900000335.
[59] P.P. Levin, A.V. Kuzmin, Laser photolysis study of triplet exciplexes of chloranil with naphthalenes, Chem. Bull. Int. Ed. (Bull. Acad. Sci. USSR, Div. Chem. Sci.). 3 (1998) 515–519. https://doi.org/https://doi.org/10.1007/BF00965347.
[60] M. Valero, P.P. Levin, N.B. Sultimova, J.E. Houston, Photochemistry of nabumetone in aqueous solution of sodium dodecyl sulfate (SDS) micelles, J. Mol. Liq. 319 (2020). https://doi.org/10.1016/j.molliq.2020.114093.
[61] N. Canudas, J. Moulinier, D. Zamora, A. Sánchez, Photobiological properties of nabumetone (4-[6-methoxy-2-naphthalenyl]-2-butanone), a novel non-steroidal anti-inflammatory and analgesic agent, Pharmazie. 55 (2000) 282–285.

Figure Captions

Figure 1: Plot of the ratio of NP fluorescence intensity in water, F_0, and that in the presence of different SDS concentrations (all of them above cmc) at emission wavelength λ_{em}=355 nm, at 20ºC. *Inset*: the plot of NP (0.04 mM) fluorescence quantum yield, ϕ_{fl} vs SDS concentration.

Figure 2: **A:** The plot of the ratio of NP solubility in SDS and in water vs. SDS volume fraction, ϕ_{SDS}, at different pHs; **B:** plot of the slope of the curves in A (partition coefficient, P, (S4)) vs. NP ionization degree X_{NP}-. At 20ºC.

Figure 3: Small-angle neutron scattering data of SDS micelles free (circles and triangles) and loaded with 1 mM NP (diamonds and squares), at 0.05 M (○,◊) and 0.2 M (Δ, □) of SDS concentration, in D_2O at 25 ºC. **A:** free and loaded micelles curves at both SDS concentrations. **B:** NP curves as in A, but with the fits (solid lines) to the ellipsoidal micelle model [31,32].

Figure 4: Fluorescence spectra of 1 mM NP at different irradiation times in: **A:** water, and **B:** 0.2M SDS. *Insets*: plots of the intensity of the bands corresponding to NP at λ_{em}=355 nm (F_{355}) and the photoproduct at λ_{em}=440 nm (F_{440}) vs. the irradiation time. The black lines correspond to the fittings of the data to a zero order kinetic. The spectra were obtained with λ_{exc}= 317 nm.

Figure 5: UV-vis transient absorption spectra of intermediates obtained upon laser flash photolysis of aerated aqueous solutions of NP (1 mM) in the presence of SDS (0.2 M) in 0.02 **(1)**, 0.25 **(3)** and 15 **(4)**, μs after the laser pulse and **(2)** is the difference of absorption spectra (1) and (3) representing the absorption spectra of e_{aq}.

Scheme 1: Chemical structure of: **(1)** anionic form of naproxen (**NP**) (sodium -2-(6-methoxynaphthalen-2-yl) propanoate and the photoproducts: **(2)** (6-methoxy-2-(1-hydroxyethyl) naphthalene, and **(3)** 6-methoxy-2-acetyl-naphthalene.